PLOS Computational Biology

RESEARCH ARTICLE

Nonlinear effects of noise on outbreaks of mosquito-borne diseases

Kyle J. -M. Dahlin[1,2*], **Karin Ebey**[3], **John E. Vinson**[1,4], **John M. Drake**[1,5]

1 Odum School of Ecology and Center for the Ecology of Infectious Diseases, University of Georgia, Athens, Georgia, United States of America, **2** Department of Mathematics, Virginia Polytechnic Institute and State University, Blacksburg, Virginia, United States of America, **3** Department of Biology, Eckerd College, St. Petersburg, Florida, United States of America, **4** Center for Wildlife Sustainability Research, Southern Illinois University, Carbondale, Illinois, United States of America, **5** Pandemic Sciences Institute, University of Oxford, Oxford, United Kingdom

* kydahlin@gmail.com

OPEN ACCESS

Citation: Dahlin KJ--M, Ebey K, Vinson JE, Drake JM (2026) Nonlinear effects of noise on outbreaks of mosquito-borne diseases. PLoS Comput Biol 22(4): e1013466. https://doi.org/10.1371/journal.pcbi.1013466

Editor: Katharina Kusejko, University Hospital Zurich, SWITZERLAND

Received: August 22, 2025

Accepted: March 24, 2026

Published: April 13, 2026

Data availability statement: The research uses no data. The R and Julia code used to conduct analyses and generate figures can be accessed at https://github.com/DrakeLab/dahlin-noisy-mbds.

Funding: We acknowledge funding from the National Science Foundation (DBI-1659683 to J.M.D) through the Population Biology of

Abstract

Mosquito-borne diseases are a significant and growing public health burden globally. Predictions about the spread and impact of mosquito-borne disease outbreaks can help inform direct control and prevention measures. However, climate change is expected to increase weather variability, potentially shaping the future of mosquito-borne disease outbreaks globally. In this study, we sought to determine the effects of demographic and environmental noise (stochasticity) on the duration and size of outbreaks predicted by models of mosquito-borne disease. We developed a demographically and environmentally stochastic Ross-Macdonald model to assess how noise affects the probability of an outbreak, the peak number of cases, and the duration of outbreaks at increasing levels of the basic reproduction number (R_0) and environmental noise strength. Increasing environmental noise reduces the risk of endemic disease from 100% down to almost 0%, but the largest outbreaks occur at intermediate environmental noise levels. In this case, if an outbreak dies out, it ends quickly. In the presence of noise, R_0 alone is insufficient to definitively predict whether an outbreak occurs. Surprisingly, our modelling results suggest that the dramatic effect on mosquito populations from increases in the frequency of extreme environmental conditions could reduce the risk of endemic disease and epidemics in some settings.

Author summary

Climate change is expected to cause drastic changes in the spread of mosquito-borne disease outbreaks, both in where they occur and in their size. A key aspect of climate change is an increase in the variability of weather factors, such as rainfall and temperature, whichalso play a crucial role in mosquito survival and reproduction. We created a mathematical model to help us understand

Infectious Diseases Undergraduate Research program. The funders had no role in study design, data collection and analysis, decision to publish, or preparation of the manuscript.

Competing interests: The authors have declared that no competing interests exist.

how increases in variability might affect future mosquito-borne disease. Results from our modeling suggest that, depending on current levels, future increases in environmental variability could either increase or decrease the size of future outbreaks. Our work highlights the need to better understand the connections between environmental changes and mosquito biology to inform efforts to forecast and suppress mosquito outbreaks.

Introduction

Mosquito-borne diseases are a significant and growing public health concern globally, with diseases such as dengue and malaria infecting over half a billion people, causing over half a million deaths annually [1–3]. Vector-borne diseases account for approximately 20% of all newly emerging infectious diseases in humans [4, 5]. The rate of emergence and spread of vector-borne diseases is increasing due to land-use and climate change, potentially exposing new populations to these diseases more frequently [6].

Anthropogenic climate change has already altered and increased the variability in temperature and precipitation and is expected to do so even more in the future [7, 8]. Alongside these climatic changes, the likelihood of extreme weather events such as droughts, heat waves, and extreme rainfall has increased on global and regional scales [9, 10]. Climate change and land-use change drive shifts in mosquito species distributions and disease emergence patterns while altering disease transmission dynamics in complicated ways [11]. For example, disease transmission is sensitive to several mosquito and pathogen traits (such as development rate, mortality rate, and biting rate) that are dependent on temperature, often in non-linear ways, leading to disease dynamics that are strongly driven by temperature [12, 13]. A major obstacle to anticipating the effects of climate change on disease is a poor understanding of the particular form of the non-linear thermal relationship between vector and parasite traits and temperature across species and in different geographic areas [14]. This complexity is evident in empirical studies: a systematic review of the correlation between temperature and dengue transmission found that dengue peaked at intermediate temperatures [15]. In another example, the temporal scale of temperature variation, in this case, daily temperature fluctuations, was found to be a key factor in determining the risk of malaria spread, highlighting the limitations of solely considering average temperature when projecting disease risk [16].

Predicting the spread and impacts of mosquito-borne diseases through mathematical and statistical models can help to inform control and prevention measures. Models have played an instrumental role in improving our understanding of mosquito-borne disease transmission and in determining the optimal targets for control for over a century [17]. Since models are often used to inform public health policies that affect community well-being and mortality rates, modelers strive to make accurate predictions by developing models that can incorporate the biological and social drivers of transmission [18, 19].

Environmental variability has long been considered to be an important driver of disease outbreaks and persistence and, more generally, in the stability of ecological networks [20–23]. For example, in some situations where modeling suggests minimal malaria transmission based on mean temperatures, daily temperature variations allow for substantial spread [16]. Demographic stochasticity refers to the inherent randomness in demographic processes like birth, death, and reproduction [24]. Environmental stochasticity refers to unpredictable variation in the environmental factors that regulate demographic processes [24, 25]. Past studies have found that ignoring environmental and demographic stochasticity may produce dynamics that do not realistically represent observed patterns in nature, presenting problems for the development of appropriate response strategies [26–28]. The influence that environmental and demographic stochasticity have on the outbreak potential and dynamics of mosquito-borne diseases remains underexplored.

Stochastic models have become more prevalent in public health and ecological research in recent decades as new analytical tools have been developed and improvements to software and hardware have made simulations more practical [29–31]. Like deterministic models, stochastic models can provide predictions of the dynamics of epidemics, including the size and timing of outbreaks [32]. Integrating stochasticity into mathematical models may prove particularly useful for studying the spatial spread of infectious diseases [33]. Stochastic models can provide probabilistic predictions of outbreak occurrence (compared to the binary predictions of deterministic models) as well as the distributions of outbreak sizes and timing by introducing noise that can influence important biological processes for transmission [34, 35]. Early warning signals, or statistics derived from noisy epidemic trajectories, can also be used to predict future system states [36–40].

Tools for stochastic modeling of mosquito-borne disease include deterministic models with random parameters [41], stochastic differential equations [27, 40], continuous- and discrete-time Markov chain simulation models [42–44], and individual-based models [45–48]. In addition to these mechanistic models, statistical modelers have considered the effects of environmental noise on disease transmission, particularly for vector-borne diseases, using species distribution models [49, 50]. Mechanistic models can be used to improve the accuracy of predictions from statistical models by identifying which parameters are most important in determining the system dynamics [51]. While many researchers have considered the effects of stochasticity on mosquito-borne disease outbreaks generally (e.g., its effect on disease emergence), the effect of environmental noise in particular on the characteristics of outbreaks has not been explored.

We modified the Ross-Macdonald mosquito-borne disease model [17, 40] to include environmental and demographic noise to explore the dynamics of mosquito-borne diseases in response to stochasticity (Fig 1). By assessing how varying levels of environmental noise affect disease outbreaks, we addressed the following questions: 1) How do demographic and environmental noise affect the probability, intensity, and duration of mosquito-borne disease outbreaks?; and 2) How does the strength of environmental noise affect the probability, intensity, and duration of mosquito-borne disease outbreaks? To explore how the magnitude of environmental noise influences key features of disease dynamics, we focused on three quantities that capture the probability and size of outbreaks: the probability of an outbreak of over 100 cases, the peak number of cases, and the duration of the outbreak.

Results

We begin by describing solutions to the deterministic submodel, then proceed to examine the results of the full model with both types of noise, and finally, to better understand the individual effects of demographic and environmental stochasticity, we consider the demographic noise and environmental noise submodels. We then separately examine the impact of varying the magnitude of environmental noise, σ, on the quantities of interest when demographic stochasticity is included or excluded.

Deterministic submodel

Consistent with standard theory, in the deterministic submodel, the probability, intensity, and duration of outbreaks depended on R_0 in a predictable manner: monotonic increase to an endemic stable state ($R_0 > 1$) or monotonic decrease

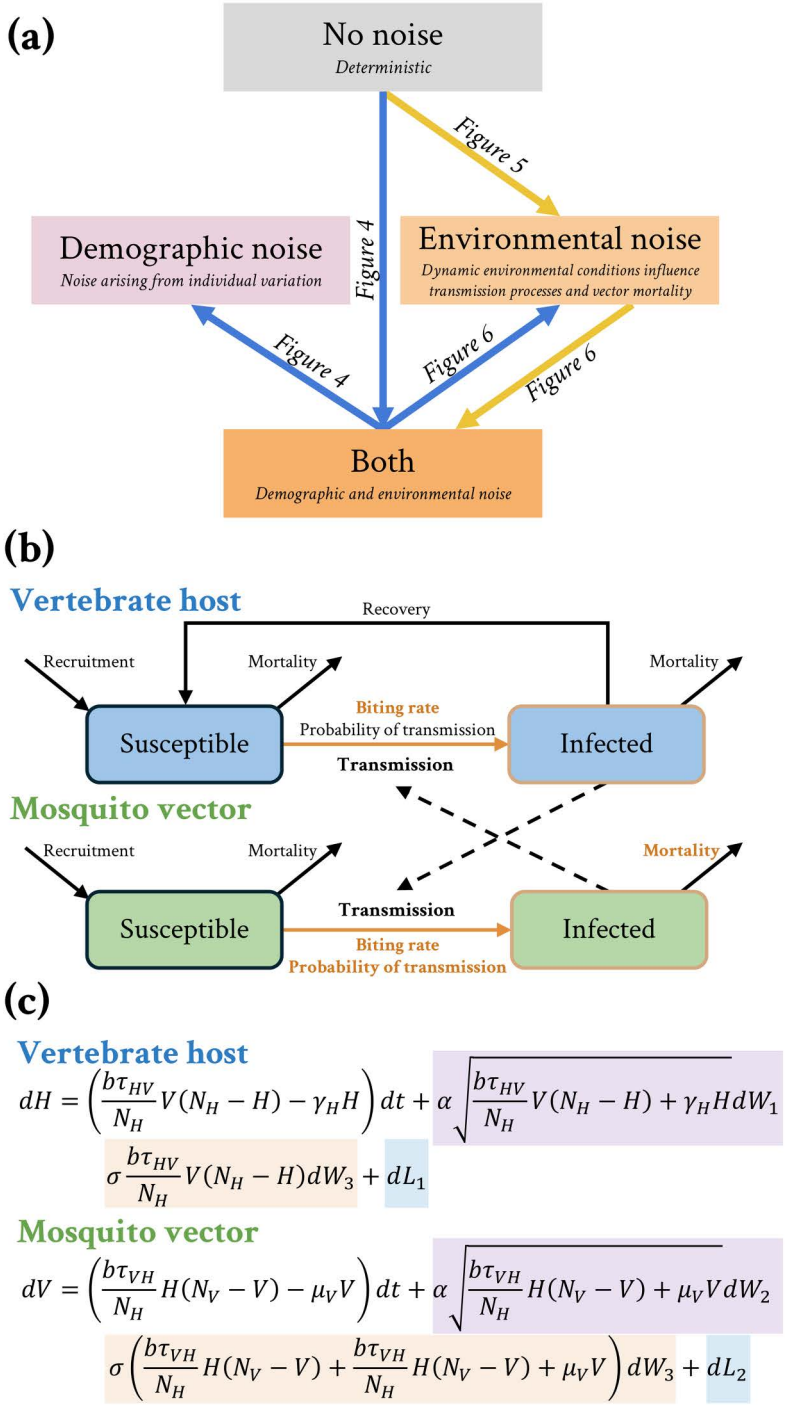

Fig 1. Conceptual diagram. (a) A conceptual diagram of the study highlighting the hierarchical nested layout of the various models. Lines represent the flow of questions explored. (b) Compartmental diagram for the model incorporating demographic and environmental stochasticity. Orange highlights indicate parameters assumed to be impacted by environmental noise. (c) Purple highlights indicate demographic stochasticity, which impacts processes, whereas orange indicates environmental stochasticity, which affects specific model parameters, also colored in orange; the probability of a susceptible host becoming infected given contact with an infectious vector, τ_{HV}, is varied so that R_0 ranges from 0.75 to 6.5. Total host and vector population sizes are fixed at their base value, while the relative numbers of infected hosts (H) and mosquito vectors (V) vary over time. The blue highlights represent the reflective processes that keep the model within a biologically meaningful space.

https://doi.org/10.1371/journal.pcbi.1013466.g001

to pathogen extinction ($R_0 < 1$) (Figs 2-black lines; 3C, 4C, and 5C "Deterministic submodel"). When $R_0 > 1.01$, an outbreak occurred where at least 1% of the host population was concurrently infected. Intensity increased monotonically with R_0, with approximately 85% of the host population becoming infectious when $R_0 = 4$ (Figs 2; black lines; and 4C "Deterministic submodel").

The addition of demographic and environmental stochasticity

Full Model. The addition of demographic and environmental noise led to the possibility of small outbreaks (on the order of 10 cases) lasting up to a year, even when R_0 was less than one (Figs 2: bottom row, orange lines; 3A, and 3B). In the deterministic submodel, the probability of a large outbreak is 100% when R_0 exceeds 1.01, but demographic and environmental noise reduce this probability, particularly as the strength of environmental noise increases (Fig 3A and 3B). While the probability of an outbreak often increased with R_0 (Fig 3A), the relationship was mediated by σ (See next section).

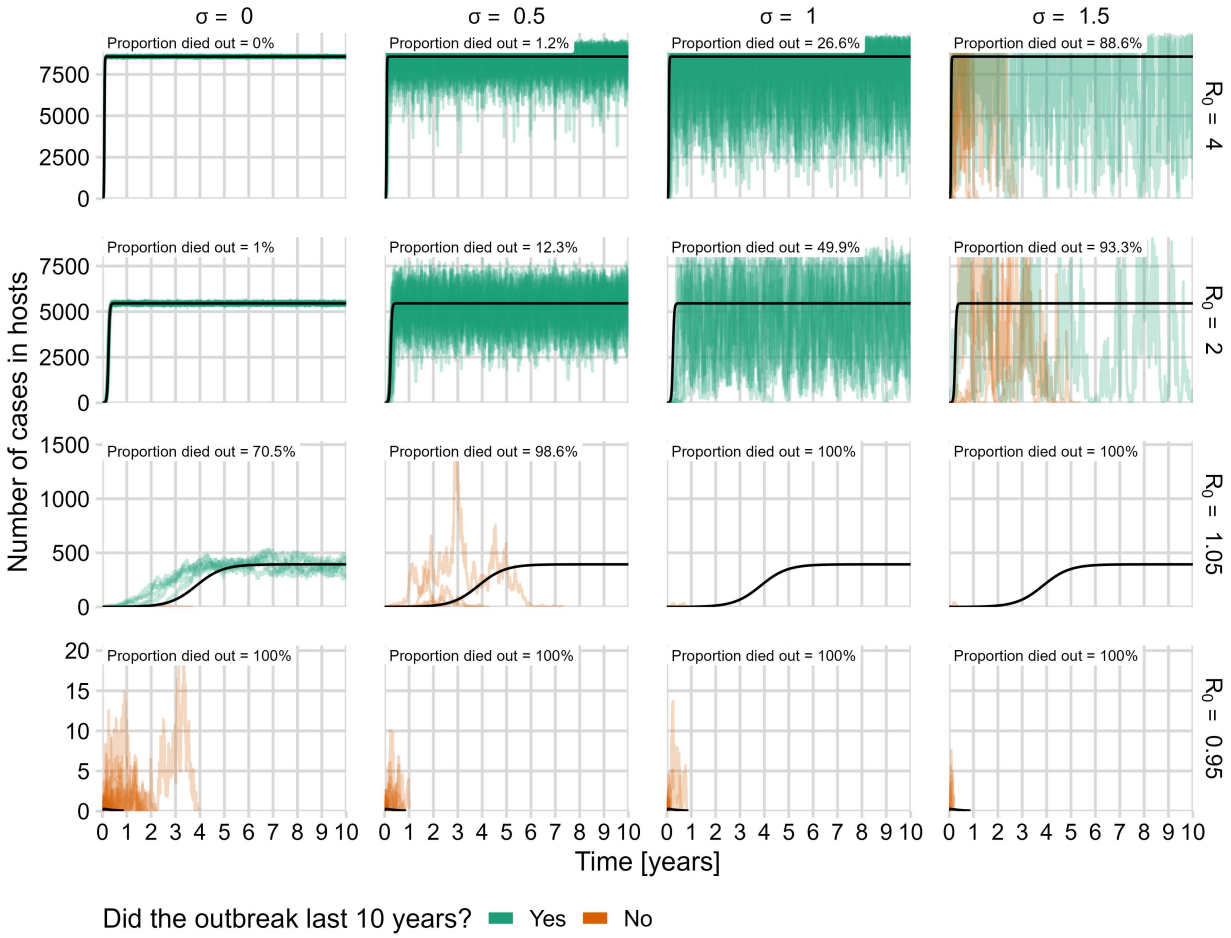

Fig 2. Deterministic model dynamics and 100 sample stochastic trajectories, including both demographic and environmental noise. The number of hosts infected throughout the ten year simulation period is plotted for 16 combinations of four environmental noise levels, (columns) and four R_0 values (rows). The black line is the deterministic result for each R_0 value. Green lines are stochastic model trajectories in which endemic disease was achieved (outbreaks persisted for the entire ten year span of simulations), and orange lines are trajectories in which the disease died out before the simulations ended. Each panel includes the proportion of simulations in which the disease died out within ten years.

https://doi.org/10.1371/journal.pcbi.1013466.g002

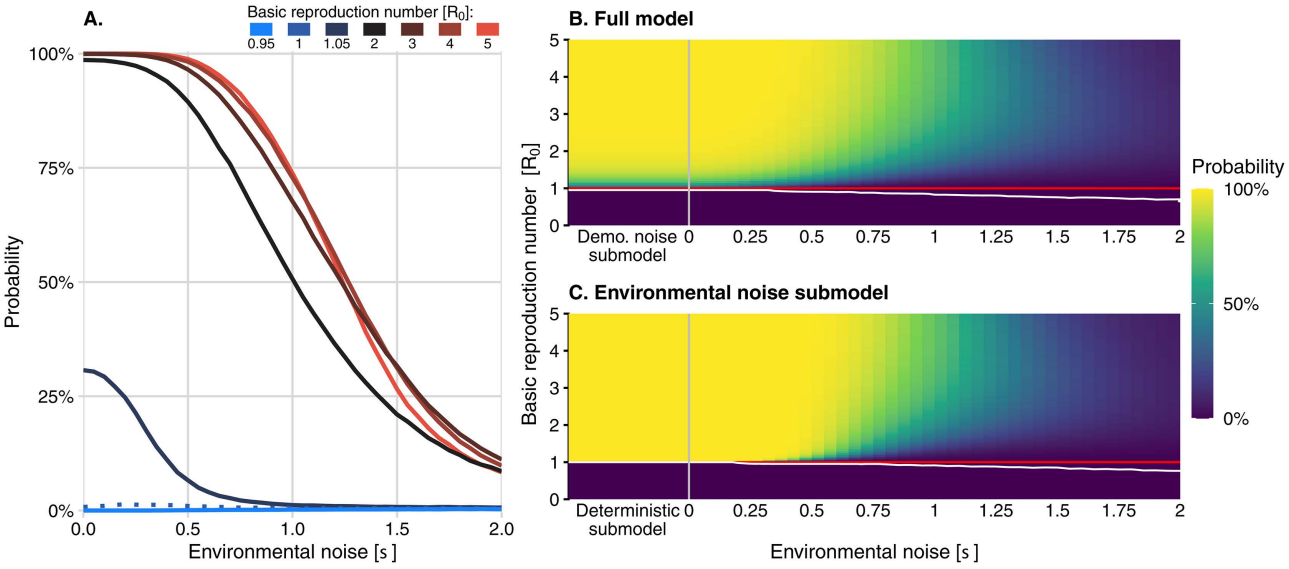

Fig 3. Probability of a large outbreak (mean of the probability of an outbreak exceeding one hundred cases in ten years across 100,000 simulations). (A) The mean of the probability of an outbreak exceeding one hundred cases in ten years across 100,000 simulations as a function of environmental noise strength for seven different R_0 values (one case in blue and the cases in red shades). The curve for R0 = 1 is indicated with a dotted line. (B) The probability of a large outbreak in the full model and (C) in the environmental noise submodel, as both environmental noise strength and the basic reproduction number are varied. The red line indicates the critical threshold of $R_0 = 1$, and the white curve indicates the contour above which the probability of an outbreak exceeds 1%. The demographic noise and deterministic submodels are shown to the left of the grey vertical lines in (B) and (C), respectively, where they are equivalent to the cases where equals zero.

https://doi.org/10.1371/journal.pcbi.1013466.g003

Increasing R_0 resulted in large oscillations in the number of host cases, typically around the number predicted by the deterministic model (Fig 2). For $R_0 = 1.05$, the host cases ranged from close to 0% up to 5% of the population, depending on the value of σ. We observed that at high values of R_0, the entire host population could become infected when σ was high (Fig 2). Inconsistent with the deterministic model, the average intensity was nonmonotonic with R_0, and peaked when σ was approximately 0.5 (Fig 4A). Average intensity was non-monotonic in both R_0 and σ (Fig 4B).

For all R_0 values, the inclusion of both demographic and environmental noise reduced the average outbreak duration compared to the deterministic submodel (Fig 5A). For low values of σ, higher R_0 resulted in longer outbreaks, but when σ was particularly high, duration dropped precipitously, and presented a non-monotonic relationship to R_0 (Fig 5B). Threshold-like behavior occurs with duration decreasing from ten years to less than a day as σ increases from 0.5 to 1.5 for R_0 values exceeding one.

Demographic noise submodel. For R_0 slightly less than one, the inclusion of demographic stochasticity led to more infected hosts compared with the deterministic submodel, but very rarely enough to cause an outbreak of over one hundred cases (Fig 3B, "Demo. noise submodel"). However, when R_0 was increased above one, demographic noise reduced the outbreak probability compared to the deterministic submodel (Figs 3B and 6A, "Difference from deterministic submodel"). Outbreak intensity consistently increased with R_0 (Fig 4B). Adding demographic stochasticity to the deterministic submodel could cause a slight increase or decrease in outbreak intensity (Fig 6B; "Difference from deterministic submodel"). For all values of $R_0 > 1$, the addition of demographic stochasticity resulted in a shorter outbreak duration compared to the deterministic submodel, particularly for values of R_0 slightly greater than one (Fig 6C "Difference from deterministic submodel"). Higher R_0 values were associated with longer-lasting outbreaks, on average.

Environmental noise submodel. The number of infected hosts in the weakly subcritical environmentally stochastic model (R_0 slightly less than one) often exceeded the number in the deterministic submodel. Still, these outbreaks were

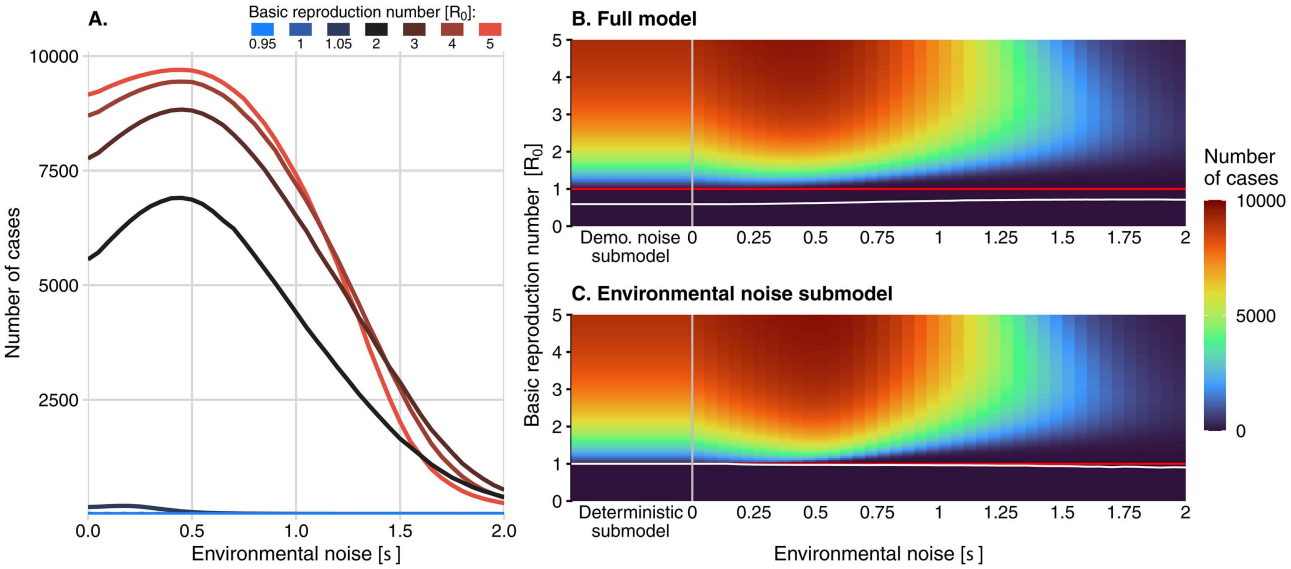

Fig 4. Intensity of outbreaks (mean of the peak number of cases attained in ten years across 100,000 simulations). (A) The mean of the peak number of host cases attained in ten years across 100,000 simulations as a function of environmental noise strength for seven different R_0 values (one case in blue and the cases in red shades). (B) The intensity of an outbreak in the full model and in the environmental noise submodel (C) as environmental noise strength and the basic reproduction number are varied. The red line indicates the critical threshold of $R_0 = 1$, and the white curve indicates the contour above which intensity is greater than a single host case. The demographic noise and deterministic submodels are shown to the left of the grey vertical lines in (B) and (C), respectively, where they are equivalent to the cases where equals zero.

https://doi.org/10.1371/journal.pcbi.1013466.g004

rarely large enough to meet our definition (Fig 3C). In general, the probability of an outbreak occurring was higher for larger values of R_0. Environmental noise caused a decrease in the probability of an outbreak for values of R_0 greater than one relative to the deterministic submodel, with a substantial increase in this effect at large values of R_0 (Fig 6A). In the environmental noise submodel, the average outbreak intensity also had a non-monotonic relationship to R_0, but outbreak intensity increased with R_0 at low values of σ (Fig 4C). Adding environmental stochasticity to the deterministic submodel reduced outbreak duration (Fig 5C).

The effect of environmental noise, σ

Environmental noise submodel. The trends observed in the environmental noise submodel, which includes environmental stochasticity but not demographic stochasticity, were largely similar to the trends in the full model, described below.

Full model. In the full model, the outbreak probability decreased with increasing σ (Fig 3A) when R_0 exceeded one. For values of σ less than approximately 1.25, higher values of R_0 led to higher outbreak probabilities. However, for all values of σ greater than 1.25, as in the environmental noise submodel, there was a non-monotonic relationship between outbreak probability and R_0 (Fig 3B). This pattern was especially evident with sharper declines as R_0 approaches its maximum value.

The demographic noise submodel exhibited smaller outbreak probabilities than the full model for small values of σ, but slightly greater outbreak probabilities for very large values of σ (Fig 6A). The shift from negative to positive impact of demographic noise on outbreak probability occurs near $\sigma = 1$ where the overall probability of an outbreak is approximately 50%.

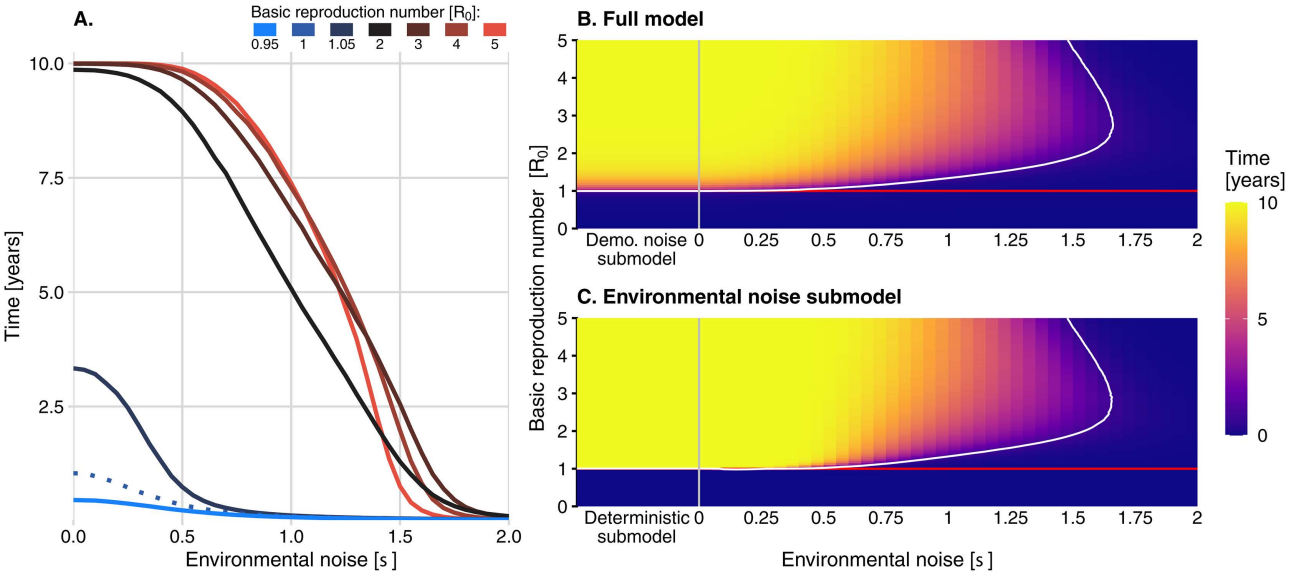

Fig 5. Duration of outbreaks (mean of the final time where there were infections in at least one host and vector across 100,000 simulations). (A) The mean of the final time at which there were infections in at least one host and vector across 100,000 simulations, plotted as a function of environmental noise strength for seven different R_0 values (one case in blue and the cases in red shades). The curve for $R_0 = 1$ is indicated by a dotted line. (B) The duration of an outbreak in the full model and (C) in the environmental noise submodel, as environmental noise strength and the basic reproduction number are varied. The red line indicates the critical threshold of $R_0 = 1$, and the white curve indicates the contour above which the duration exceeds one day. The demographic noise ("Demo. noise submodel") and deterministic submodels are shown to the left of the grey vertical lines in (B) and (C), respectively, where they are equivalent to the cases where equal zero.

https://doi.org/10.1371/journal.pcbi.1013466.g005

Intensity had a non-monotonic relationship with σ (Fig 4A). Across all values of R_0, the maximum intensity occurred at intermediate values of σ, ranging from 0.4 to 0.6. When σ is less than 1.25, increasing R_0 led, on average, to a higher outbreak intensity (Fig 4B). However, when σ exceeded 1.25, increasing R_0 instead caused a decrease in intensity. Comparing the complete model to the environmental noise submodel revealed that the effect of demographic noise on outbreak intensity depended on σ, resulting in lower outbreak intensity at low σ when R_0 exceeded one, but slightly higher values when σ was high (Fig 6B).

Increasing σ resulted in shorter average outbreak durations (Fig 5A). For $\sigma < 1.25$, increasing R_0 resulted in longer average outbreak durations, while at higher values of σ duration had a non-monotonic relationship to R_0 (Fig 5B). The effect of adding demographic noise on outbreak durations was similar to its effect on intensities (Fig 6C).

Distributions of intensity and duration across simulations. To better understand how the distributions of intensity and duration vary, we calculated them for select combinations of R_0 and σ. At low σ and R_0, the pathogen immediately went extinct, with no individuals becoming infected (Fig A in S1 Text, bottom-left plot). However, when the pathogen was able to persist, intensity varied widely. Increasing σ resulted in more simulations in which the pathogen quickly went extinct, but again, outbreaks that persisted had a wide range of intensities (Fig A in S1 Text, bottom-right plot). Large values of R_0 resulted in a bimodal distribution of intensity where either the pathogen goes extinct quickly with very few individuals infected or persists, and every individual becomes infected (Fig A in S1 Text, top-left plot). On the other hand, increasing $\sigma\sigma$ led to an increase in the number of simulations in which the pathogen went extinct, but for those short simulations, the intensity was commonly very high (Fig A in S1 Text, top-right plot).

The reduction in the average outbreak duration with $\sigma\sigma$ was mainly due to simulations where the pathogen went extinct nearly instantly (Fig A in S1 Text). At lower R_0, the pathogen often went extinct immediately, but in some simulations, the duration spanned from zero to ten years. With low σ and high R_0, the pathogen extinction occurred within days or

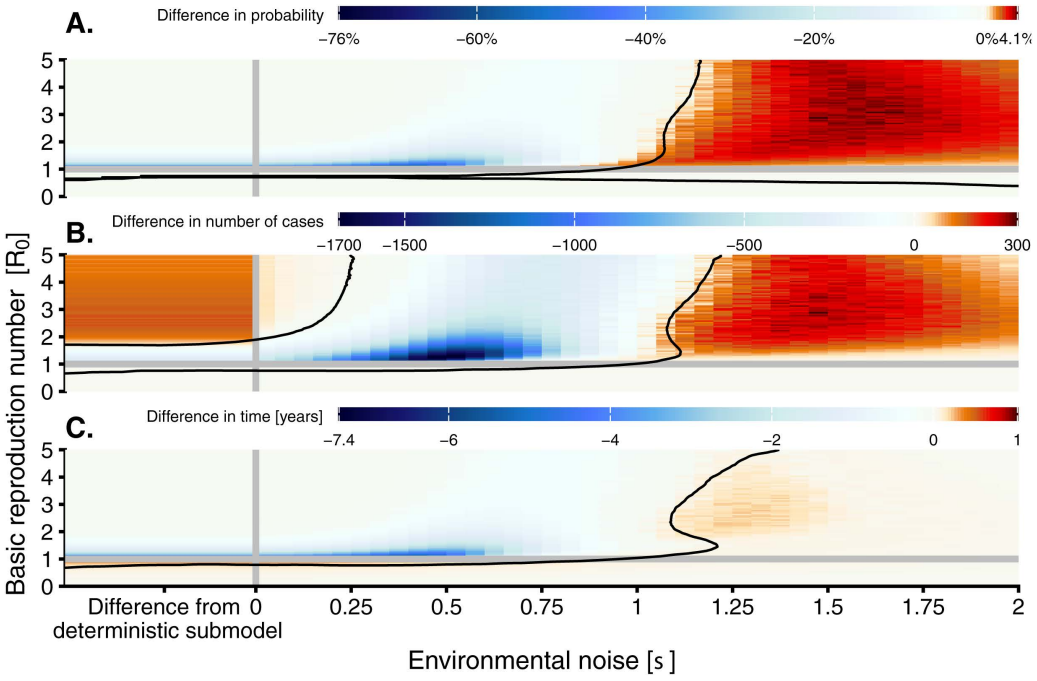

Fig 6. Heatmaps of the difference in probability (A), average intensity (B), and average duration (C) of an outbreak between the full model with both demographic and environmental noise and the environmental noise submodel (i.e., the difference in the values between subplots (B) and (C) in the Figs 3, 4, and 5, respectively). The leftmost side of each heatmap indicates the difference between the deterministic submodel and the demographic noise submodel ("Difference from deterministic submodel"). The horizontal grey line indicates the critical threshold of $R_0 = 1$, and the black contour lines separate approximate regions of positive and negative differences.

https://doi.org/10.1371/journal.pcbi.1013466.g006

persisted for ten years. For lower R_0 and high σ, the pathogen often became established in the population, but outbreaks lasted only a short time, and none persisted for the entire ten-year period (Fig A in S1 Text, bottom-right plot). At high R_0 and σ, outbreaks could last for brief periods, as the pathogen went extinct immediately. Still, there was potential for the pathogen to persist the entire 10-year period (Fig A in S1 Text, upper-right plot). In this case, simulations had intense outbreaks (a high number of host infections) but short durations (lasting less than 2.5 years). This highlights that the mean values of stochastic trajectories do not provide a complete picture of the possible dynamics, as some trends show bimodality or fail to capture the potentially important "extreme" cases (e.g., short but intense outbreaks).

Discussion

Our results indicate that the effects of demographic and environmental stochasticity on three key measures of an outbreak (probability, intensity, and duration) may be nonlinear. The presence of demographic and environmental stochasticity, alone or together, could reduce the probability and duration of outbreaks compared to models with a single source of stochasticity or none, with further reductions observed as environmental noise increases. With our stochastic model describing mosquito-borne pathogen transmission, we found that demographic and environmental stochasticity interact to create conditions unfavorable for outbreak persistence, even when $R_0 > 1$. It is intuitive that demographic stochasticity can reduce outbreak persistence because transmission relies on sufficient interactions between two populations, both of which may be negatively affected by demographic stochasticity. But the mechanism by which environmental stochasticity can drive decreases in outbreak persistence is less clear.

Our finding of the non-monotonic relationship between environmental noise and average outbreak intensity is consistent with observed nonlinear responses between the environment (e.g., temperature) and biological processes for vector-borne parasite transmission (e.g., biting rate) [12]. Daily temperature fluctuations have been shown to control the transmission dynamics of vector-borne parasites, such as the longevity of mosquitoes infected with dengue virus [52, 53], viral loads of West Nile virus [54], and several rates associated with malaria transmission [55]. However, others have found that daily temperature variation can have little to no effect on viral load in vectors [56] or infectivity and susceptibility [54]. Our model is limited by the assumption that environmental fluctuations equally and proportionally affect the vector biting rate, mortality rate, and the ability of mosquitoes to pass the pathogen on to hosts, all of which may be non-linearly correlated with environmental variables like temperature, rainfall, and humidity [57]. In addition, while we assume that environmental changes do not impact hosts, such changes are likely to have different and meaningful impacts on both hosts and vectors. For example, hotter temperatures could have counteracting effects on transmission by increasing intrinsic mosquito biting rates while also driving more people indoors.

Our results shed light on the potential implications of more extreme environmental variation on outbreak intensity. Outbreaks may become more intense with increased environmental variation, but this might depend on whether current levels of environmental variation are sufficiently low. Generally, researchers expect that increased environmental fluctuations will lead to more outbreaks [6]. However, counterintuitively, in our modelling results, the opposite effect occurs at higher levels of environmental variation, where the environment occasionally strongly increases mosquito mortality or decreases transmission competency, leading to pathogen extinction. It is important to note that in our model, σ is a simplified composite variable that represents the total effect of environmental variation on key mosquito traits; it does not directly capture the nonlinear effects of environmental factors, such as temperature or rainfall, on these traits. However, if increases in environmental variation are expected to lead to more extreme effects on mosquito traits, then σ may be a reasonable proxy.

The observed shift in the relationships between the outbreak measures and R_0 when σ is large might be explained by early crashes in the infected mosquito population when the number of infected hosts is small. Because $(H, V) = (0, 0)$ is an absorbing state of the model, if both forms of noise have a strong negative effect at the start of an outbreak, they can quickly push both infected populations to zero. This phenomenon is an intrinsic property of the stochastic processes and reflection processes incorporated into system (2). When both R_0 and σ are large, the environmental stochasticity terms (i.e., those that include dW_3) can be both large and negative in a single timestep. To ensure that trajectories remain in the biologically feasible domain, the reflection terms will then send both trajectories to zero. When there are no infectious cases in either hosts or vectors, the outbreak necessarily dies out. Instead of using stochastic differential equations, future work could use a discrete-time Markov chain model with non-Gaussian increments in the stochastic terms, for example, truncated normally-distributed increments, that ensure the trajectories can never become negative in a single timestep.

In models with demographic and environmental noise, outbreak probability, intensity, and duration generally increased with R_0. This is consistent with our deterministic model, where the equilibrium outbreak intensity depends on R_0. However, we found a non-monotonic relationship between R_0 and all three disease outcomes, with the outbreak probability, intensity, and duration being highest at intermediate R_0 values. As described previously, at higher values of R_0 and σ, the pathogen may be more susceptible to stochastic extinction. Previous work has shown that, for stochastic models, the probability of an outbreak is $1 - (1/R_0)^i$, where i is the initial number of infectious individuals [58]. This result can be extended to models with multiple infectious compartments [32]. However, while these stochastic models suggest that increasing R_0 increases outbreak probabilities, our findings suggest that environmental stochasticity can disrupt this relationship when R_0 is large.

Our detailed study of the distributions of outbreak intensity and duration at various R_0 and σ values revealed that changes in their average values were due to bimodality in their distributions. As σ was increased, more simulations underwent immediate pathogen die-out than simulations with no or low environmental noise, leading to decreases in the average intensity and duration values. Thus, when σ is sufficiently high, there is a substantial divergence in outbreak outcomes where either the pathogen dies out quickly, infecting very few individuals, or the outbreak persists, so that many

individuals become infected. Averages are generally used to summarize unimodal distributions, as they provide a standardized value for comparing groups assumed to be normally distributed. However, as we observed here, the distributions of our quantities of interest were bimodal. These results reinforce the idea that the public health implications of increased environmental variability will be nuanced. Increasing environmental noise could increase the probability of outbreaks dying out quickly. But if outbreaks do become established in a population, they could be just as severe and last as long as outbreaks that occur with low variability. Stochastic models of mosquito-borne disease transmission without environmental stochasticity exhibit early warning signals that predict the end of an epidemic [40]. By analyzing the stochastic trajectories preceding the divergence into outbreak persistence or elimination, future work could investigate whether early warning signals for disease elimination exist when environmental stochasticity is included.

Our aim was to isolate the effects of noise on mosquito-borne disease dynamics from other factors that may influence our metrics of interest. To do so, we started with a straightforward yet traditional model of mosquito-borne pathogen transmission [17]. However, this simple model relies on several simplifying assumptions. Critically, daily, seasonal, and annual environmental variations are not considered. One limitation is the lack of mosquito life stages, including their aquatic stages, which are extremely sensitive to environmental conditions such as precipitation and humidity. Extrinsic incubation periods, which are also sensitive to temperature and are critical indicators of persistence of some pathogens like malaria, were also excluded from the model [12, 59]. Temperature and humidity are also known to affect life-history traits of parasites, such as *Plasmodium* malaria, and the transmissibility of viruses [12]. A more detailed model would include environmental responses to additional vector life history traits and pathogen traits, better representing the mechanistic relationships between vector life history and variation in abiotic factors like temperature, humidity, and rainfall. Such work could guide future disease mitigation efforts by identifying key mosquito life-history traits associated with transmission while also integrating the impacts of environmental and demographic noise on transmission.

Our study represented environmental stochasticity as a phenomenological process that proportionately impacts three mosquito life-history traits. However, the influence of environmental variables on mosquito and pathogen biological processes is non-linear and affects each trait differently, so, for example, large environmental changes could have little effect on one trait while strongly affecting another. Realistically, environmental factors cannot be grouped into a single effect, as the interactions between factors strongly affect mosquito life history traits (e.g., humidity most strongly affects mosquito trait performance at higher temperatures) [57]. An analysis of the type presented here would be computationally infeasible for an entirely mechanistic and stochastic model of mosquito-borne disease transmission that incorporates realistic environmental variation. However, through comparison to the results presented here, such a model could be used to better understand how outbreaks are affected by separate environmental factors and their link to mosquito life history traits.

While environmental variation is understood to influence many ecological processes, in particular those involving insects [60–63], it is not commonly incorporated into models of mosquito-borne disease transmission. Our study yielded nuanced and counterintuitive insights into how demographic and environmental stochasticity determine key features of an outbreak: probability, intensity, and duration. In a world experiencing increases not only in average temperatures but also in the amount of variation of such environmental factors, stochastic modeling can be used to predict the distribution of possible futures, improving our understanding of the effectiveness of disease intervention and prevention measures. If the burden of mosquito-borne disease increases and shifts as our planet's climate changes, it is crucial that we understand the potential non-intuitive and nonlinear effects of a more variable world on the fate of outbreaks.

Methods

Model

We studied a system of stochastic differential equations (SDE), a version of the Ross-Macdonald compartmental model of mosquito-borne disease transmission with demographic stochasticity [17]. The model is based on a system of equations previously formulated and studied by [40], but extended to include environmental stochasticity in key mosquito traits and

reflection terms to ensure that the state variables remain in the biologically feasible domain. A key assumption is that the total host and vector populations are at their positive equilibria. As a result, the only values changing are the relative proportions of infected hosts, H, and vectors, V:

$$dH = \left(\frac{b\tau_{HV}}{N_H}V(N_H - H) - \gamma_H H\right)dt + \sqrt{\frac{b\tau_{HV}}{N_H}V(N_H - H) + \gamma_H H}dW_1,$$
$$dV = \left(\frac{b\tau_{VH}}{N_H}H(N_V - V) - \mu_V V\right)dt + \sqrt{\frac{b\tau_{VH}}{N_H}H(N_V - V) + \mu_V V}dW_2, \quad (1)$$

where W_1 and W_2 are independent Wiener processes. Here, H is the number of infectious hosts, N_H is the total number of hosts, V is the number of infectious vectors, and N_V is the total number of vectors. The force of infection for hosts is given by $\frac{b\tau_{HV}}{N_H}V$ and for vectors by $\frac{b\tau_{VH}}{N_H}H$. All parameters are defined and described in Table 1.

We included environmental noise by perturbing the mortality rate μ_V, biting rate b, and transmission competency τ_{VH}, with an additional Wiener process independent to those for demographic stochasticity. These are the mosquito traits most tightly linked to environmental factors, such as temperature and rainfall [12]. Environmental variation was assumed to proportionally perturb a parameter g through the Wiener process described by $g(t)\Delta t = g_0\Delta t + \sigma g_0 \eta\sqrt{\Delta t}$, where g_0 is the value of g in the absence of environmental noise, η is the standard normal distribution, and σ denotes the strength of the effect of environmental noise on the parameter. The system of equations in Fig 1b gives the final system of stochastic differential equations. We explored σ in the range of 0, representing no environmental noise, to a maximum of 2.0, corresponding to the parameters varying up to three times their intrinsic value. The parameter α allows us to turn demographic noise on (α = 1) or off (α = 0). Environmental stochasticity approximates the effects of random or complex changes in

Table 1. Table of parameters, their definitions, and values.

Parameter	Description (Units)	Base value(Range)	References & Notes
Host transmission probability τ_{HV}	Probability of a susceptible host becoming infected given contact with an infectious vector	(0, 0.55)	Range chosen so that R_0 varies from 0.05 5.0 (see Parameterization)
Host recovery rate γ_H	Rate at which hosts recover from infection (per day)	0.1	Corresponds to an average infectious period of 10 days
Total host population size N_H	Total number of hosts	10,000	Representing the population of a small town
Biting rate b	Bites per mosquito per unit time (per day)	0.3	An average of one bite every three days, roughly corresponding with the value at the thermal optimum for *Aedes aegypti* [12]
Vector transmission probability τ_{VH}	Probability of a susceptible vector becoming infected given contact with an infectious host	0.5	Set to be the midpoint between 0% and 100%
Vector mortality rate μ_V	Rate at which vectors experience mortality (per day)	0.1	Half the minimum mortality rate for *Aedes aegypti,* corresponding to an average of ten days [12]
Total vector population size N_V	Total number of mosquito vectors	100,000	Chosen to ensure a 10:1 vector-host ratio
Environmental noise strength σ	Variance in the environmental parameters	(0, 2.0)	

The rows highlighted in orange are parameters that are influenced by environmental noise.

https://doi.org/10.1371/journal.pcbi.1013466.t001

the environment, such as temperature or rainfall. As an example of how σ relates to real-world observations, for *Aedes aegypti* and Zika or dengue virus, as temperature ranges between 20 and 40°C, biting rates are predicted to vary between 0.1 and 0.32, lifespans between zero and 42 days, and infection probability 30% to 60% [12]. These correspond to variations of 34%, 100%, and 33%, respectively (or σ = 0.3, 1, and0.33 in our model).

To ensure that solutions of the stochastic model remained in the biologically feasible domain, $D = [0, N_H] \times [0, N_V]$, which is also the invariant domain of the deterministic model, we modified the equations with reflection terms to arrive at the system of reflected SDEs (2).

$$dH = \left(\frac{b\tau_{HV}}{N_H}V(N_H - H) - \gamma_H H\right)dt + \alpha\sqrt{\frac{b\tau_{HV}}{N_H}V(N_H - H) + \gamma_H H}dW_1 + \sigma b\frac{\tau_{HV}}{N_H}V\left(N_H - H\right)dW_3 + dL_1,$$
$$dV = \left(\frac{b\tau_{VH}}{N_H}H(N_V - V) - \mu_V V\right)dt + \alpha\sqrt{\frac{b\tau_{VH}}{N_H}H(N_V - V) + \mu_V V}dW_2 + \sigma\left(\frac{b\tau_{VH}}{N_H}H(N_V - V) + \frac{b\tau_{VH}}{N_H}H(N_V - V) + \mu_V V\right)dW_3 + dL_2. \quad (2)$$

Here dL_1 and dL_2 are the stochastic processes that reflect the process into D. Solutions to system (2) exist and are unique because D is bounded [64].

Parameterization

Without stochasticity, this model admits the basic reproduction number in equation (3) derived using the next-generation method approach [65, 66].

$$R_0 = \sqrt{b^2 \times \tau_{VH} \times \frac{1}{\mu_V} \times \left(\tau_{HV}\frac{N_V}{\gamma_H N_H}\right)} \quad (3)$$

We used the basic reproduction number to determine parameter values such that the deterministic model will lead to persistent transmission ($R_0 > 1$) or disease extinction ($R_0 < 1$) by fixing all parameters except τ_{HV} then varying τ_{HV} so that R_0 varied from 0.05 to 5.0, to include values below and exceeding one, the deterministic threshold for outbreaks.

Simulations and analyses

Quantifying disease dynamics: Quantities of interest. We first conducted an exploratory analysis of model trajectories to better characterize system dynamics over 10 years (Fig 2). Simulations were initialized with ten infectious vectors, and total host and vector populations were set to their maximum values of N_H and N_V, respectively. Solutions to system (2) were approximated using the projection method for the Euler-Maruyama algorithm on the domain D with time steps of one-tenth of one day [67]. We observed that even when R_0 greatly exceeded one, outbreaks commonly died out at high levels of environmental noise.

Based on these initial observations, we chose to focus our analysis on three quantities: the probability of an outbreak (henceforth, "probability), the peak number of cases ("intensity"), and the duration of the outbreak ("duration"). Understanding these quantities could help decision-makers determine disease risk and prepare for large outbreaks in their communities [68–70]. We defined a realization of the SDE system (2) as an outbreak when the peak number of human cases exceeded 100, that is, when more than 1% of the human population was infectious. Probability was calculated as the proportion of 10,000 realizations that resulted in such an outbreak. Intensity was defined as the maximum number of hosts infected on any one day during the simulation. Duration was defined as the number of days where there was at

least one infected host during the simulation or, if the outbreak did not die out, as 10 years, the maximum duration of the simulations. Probability, intensity, and duration were calculated from 10,000 realizations of the SDE system (2).

Because of environmental and demographic stochasticity, each quantity of interest (probability, intensity, or duration) was a random variable. We calculated each quantity of interest for levels of environmental noise, σ, ranging from 0 to 2.0, and values of R_0 from 0.05 to 5, both in increments of 0.025. For each value of σ and R_0, we obtained a distribution of outcomes. To describe these distributions, we calculated their mean, median, variance, and 25% and 75% quantiles. We primarily report our results using mean values, but this approach assumes a unimodal distribution of our metrics. To investigate whether this assumption held, we explored the qualitative shape of these distributions for selected values of R_0 and σ.

Hierarchical submodels. We were interested in exploring how demographic and environmental noise can influence the probability, intensity, and duration of outbreaks. System (2) allows for either form of noise to be turned on or off through the parameters α and σ. We systematically explored four hierarchical submodels described by system (2) and outlined this process in Fig 1a. The first model included no forms of stochasticity, which we refer to as the "deterministic model" ($\alpha = 0$and $\sigma = 0$). Two models include a single form of stochasticity, the "demographic noise" model ($\alpha = 1$, $\sigma = 0$) and the "environmental noise model" ($\alpha = 0$, $\sigma \neq 0$). We also included the complete model that includes "both" forms of noise ($\alpha = 1$, $\sigma \neq 0$). For cases where $\sigma \neq 0$, we considered values of σ ranging up to 2.0.

Software. While all figures were produced in *R* (version 4.2.3), all simulations were run in the *Julia* language, which can estimate solutions to stochastic differential equations with non-diagonal noise and reflection [71, 72]. All code used to produce the results and figures in this manuscript is available in a GitHub repository maintained by the authors and located at the URL https://github.com/DrakeLab/dahlin-noisy-mbds.

Supporting information

S1 Text. Supplementary figures for Nonlinear effects of noise on outbreaks of mosquito-borne diseases. Supplementary captions from Fig A-Fig M.
(PDF)

Acknowledgments

The authors thank the participants of the Population Biology of Infectious Diseases REU at the University of Georgia for valuable feedback.

Author contributions

Conceptualization: Kyle J. -M. Dahlin, Karin Ebey, John E. Vinson, John M. Drake.

Data curation: Kyle J. -M. Dahlin, Karin Ebey.

Formal analysis: Kyle J. -M. Dahlin, Karin Ebey, John E. Vinson.

Funding acquisition: John M. Drake.

Investigation: Kyle J. -M. Dahlin, Karin Ebey, John E. Vinson.

Methodology: Kyle J. -M. Dahlin, Karin Ebey, John E. Vinson.

Project administration: Kyle J. -M. Dahlin.

Resources: John M. Drake.

Software: Kyle J. -M. Dahlin, Karin Ebey.

Supervision: Kyle J. -M. Dahlin, John M. Drake.

Validation: Kyle J. -M. Dahlin.

Visualization: Kyle J. -M. Dahlin, Karin Ebey.

Writing – original draft: Kyle J. -M. Dahlin, Karin Ebey, John E. Vinson.

Writing – review & editing: Kyle J. -M. Dahlin, Karin Ebey, John E. Vinson, John M. Drake.

References

1. World Health Organization. World malaria report 2022. Genève, Switzerland: World Health Organization. 2022.
2. Bhatt S, Gething PW, Brady OJ, Messina JP, Farlow AW, Moyes CL, et al. The global distribution and burden of dengue. Nature. 2013;496(7446):504–7. https://doi.org/10.1038/nature12060 PMID: 23563266
3. Zhang W-X, Zhao T-Y, Wang C-C, He Y, Lu H-Z, Zhang H-T, et al. Assessing the global dengue burden: Incidence, mortality, and disability trends over three decades. PLoS Negl Trop Dis. 2025;19(3):e0012932. https://doi.org/10.1371/journal.pntd.0012932 PMID: 40072961
4. Jones KE, Patel NG, Levy MA, Storeygard A, Balk D, Gittleman JL, et al. Global trends in emerging infectious diseases. Nature. 2008;451(7181):990–3. https://doi.org/10.1038/nature06536 PMID: 18288193
5. Daszak P, Cunningham AA, Hyatt AD. Emerging infectious diseases of wildlife--threats to biodiversity and human health. Science. 2000;287(5452):443–9. https://doi.org/10.1126/science.287.5452.443 PMID: 10642539
6. Chala B, Hamde F. Emerging and Re-emerging Vector-Borne Infectious Diseases and the Challenges for Control: A Review. Front Public Health. 2021;9:715759. https://doi.org/10.3389/fpubh.2021.715759 PMID: 34676194
7. Pendergrass AG, Knutti R, Lehner F, Deser C, Sanderson BM. Precipitation variability increases in a warmer climate. Sci Rep. 2017;7(1):17966. https://doi.org/10.1038/s41598-017-17966-y PMID: 29269737
8. Brown PT, Ming Y, Li W, Hill SA. Change in the magnitude and mechanisms of global temperature variability with warming. Nat Clim Chang. 2017;7:743–8. https://doi.org/10.1038/nclimate3381 PMID: 29391875
9. Field CB, Barros V, Stocker TF, Dahe Q. Managing the risks of extreme events and disasters to advance climate change adaptation: special report of the Intergovernmental Panel on Climate Change. Field CB, Barros V, Stocker TF, Dahe Q, editors. Cambridge, England: Cambridge University Press. 2012.
10. Thornton PK, Ericksen PJ, Herrero M, Challinor AJ. Climate variability and vulnerability to climate change: a review. Glob Chang Biol. 2014;20(11):3313–28. https://doi.org/10.1111/gcb.12581 PMID: 24668802
11. Lafferty KD. The ecology of climate change and infectious diseases. Ecology. 2009;90(4):888–900. https://doi.org/10.1890/08-0079.1 PMID: 19449681
12. Mordecai EA, Caldwell JM, Grossman MK, Lippi CA, Johnson LR, Neira M, et al. Thermal biology of mosquito-borne disease. Ecol Lett. 2019;22(10):1690–708. https://doi.org/10.1111/ele.13335 PMID: 31286630
13. Dahlin KJ-M, O'Regan SM, Han BA, Schmidt JP, Drake JM. Impacts of host availability and temperature on mosquito-borne parasite transmission. Ecol Monogr. 2024;94. https://doi.org/10.1002/ecm.1603
14. Altizer S, Ostfeld RS, Johnson PTJ, Kutz S, Harvell CD. Climate change and infectious diseases: from evidence to a predictive framework. Science. 2013;341(6145):514–9. https://doi.org/10.1126/science.1239401 PMID: 23908230
15. Kirk D, Straus S, Childs ML, Harris M, Couper L, Davies TJ, et al. Temperature impacts on dengue incidence are nonlinear and mediated by climatic and socioeconomic factors: A meta-analysis. PLOS Clim. 2024;3(3):e0000152. https://doi.org/10.1371/journal.pclm.0000152
16. Paaijmans KP, Read AF, Thomas MB. Understanding the link between malaria risk and climate. Proc Natl Acad Sci U S A. 2009;106(33):13844–9. https://doi.org/10.1073/pnas.0903423106 PMID: 19666598
17. Smith DL, Battle KE, Hay SI, Barker CM, Scott TW, McKenzie FE. Ross, macdonald, and a theory for the dynamics and control of mosquito-transmitted pathogens. PLoS Pathog. 2012;8(4):e1002588. https://doi.org/10.1371/journal.ppat.1002588 PMID: 22496640
18. Evans MR, Grimm V, Johst K, Knuuttila T, de Langhe R, Lessells CM. Do simple models lead to generality in ecology? Trends Ecol Evol. 2013;28:578–83. https://doi.org/10.1016/j.tree.2013.05.022
19. Bertozzi AL, Franco E, Mohler G, Short MB, Sledge D. The challenges of modeling and forecasting the spread of COVID-19. Proc Natl Acad Sci U S A. 2020;117(29):16732–8. https://doi.org/10.1073/pnas.2006520117 PMID: 32616574
20. Conlan AJK, Rohani P, Lloyd AL, Keeling M, Grenfell BT. Resolving the impact of waiting time distributions on the persistence of measles. J R Soc Interface. 2010;7(45):623–40. https://doi.org/10.1098/rsif.2009.0284 PMID: 19793743
21. Keeling MJ, Grenfell BT. Understanding the persistence of measles: reconciling theory, simulation and observation. Proc Biol Sci. 2002;269(1489):335–43. https://doi.org/10.1098/rspb.2001.1898 PMID: 11886620
22. Lande R. Risks of Population Extinction from Demographic and Environmental Stochasticity and Random Catastrophes. Am Nat. 1993;142(6):911–27. https://doi.org/10.1086/285580 PMID: 29519140

23. Ripa J, Lundberg P, Kaitala V. A general theory of environmental noise in ecological food webs. Am Nat. 1998;151(3):256–63. https://doi.org/10.1086/286116 PMID: 18811356
24. Engen S, Bakke O, Islam A. Demographic and Environmental Stochasticity-Concepts and Definitions. Biometrics. 1998;54(3):840. https://doi.org/10.2307/2533838
25. Fujiwara M, Takada T. Environmental stochasticity. eLS. Chichester, UK: John Wiley & Sons, Ltd. 2017:1–8. https://doi.org/10.1002/9780470015902.a0021220.pub2
26. Pelosse P, Kribs-Zaleta CM, Ginoux M, Rabinovich JE, Gourbière S, Menu F. Influence of vectors' risk-spreading strategies and environmental stochasticity on the epidemiology and evolution of vector-borne diseases: the example of Chagas' disease. PLoS One. 2013;8(8):e70830. https://doi.org/10.1371/journal.pone.0070830 PMID: 23951018
27. Britton T, Traoré A. A stochastic vector-borne epidemic model: Quasi-stationarity and extinction. Math Biosci. 2017;289:89–95. https://doi.org/10.1016/j.mbs.2017.05.004 PMID: 28511957
28. Reiner RC Jr, Guerra C, Donnelly MJ, Bousema T, Drakeley C, Smith DL. Estimating malaria transmission from humans to mosquitoes in a noisy landscape. J R Soc Interface. 2015;12(111):20150478. https://doi.org/10.1098/rsif.2015.0478 PMID: 26400195
29. Kuehn C. A mathematical framework for critical transitions: Bifurcations, fast–slow systems and stochastic dynamics. Physica D: Nonlinear Phenomena. 2011;240(12):1020–35. https://doi.org/10.1016/j.physd.2011.02.012
30. Nolting BC, Abbott KC. Balls, cups, and quasi-potentials: quantifying stability in stochastic systems. Ecology. 2016;97(4):850–64. https://doi.org/10.1890/15-1047.1 PMID: 27220202
31. Shoemaker LG, Sullivan LL, Donohue I, Cabral JS, Williams RJ, Mayfield MM, et al. Integrating the underlying structure of stochasticity into community ecology. Ecology. 2020;101(2):e02922. https://doi.org/10.1002/ecy.2922 PMID: 31652337
32. Allen LJS, Lahodny GE Jr. Extinction thresholds in deterministic and stochastic epidemic models. J Biol Dyn. 2012;6:590–611. https://doi.org/10.1080/17513758.2012.665502 PMID: 22873607
33. Lahodny GEJ, Allen LJS. Probability of a disease outbreak in stochastic multipatch epidemic models. Bull Math Biol. 2013;75:1157–80. https://doi.org/10.1007/s11538-013-9848-z
34. Allen LJS. An introduction to stochastic processes with applications to biology. 2nd ed. Philadelphia, PA: Chapman & Hall/CRC. 2024. https://doi.org/10.1201/b12537
35. King AA, Domenech de Cellès M, Magpantay FMG, Rohani P. Avoidable errors in the modelling of outbreaks of emerging pathogens, with special reference to Ebola. Proc Biol Sci. 2015;282(1806):20150347. https://doi.org/10.1098/rspb.2015.0347 PMID: 25833863
36. Dakos V, Carpenter SR, Brock WA, Ellison AM, Guttal V, Ives AR, et al. Methods for detecting early warnings of critical transitions in time series illustrated using simulated ecological data. PLoS One. 2012;7(7):e41010. https://doi.org/10.1371/journal.pone.0041010 PMID: 22815897
37. Drake JM, O'Regan SM, Dakos V, Kéfi S, Rohani P. Alternative stable states, tipping points, and early warning signals of ecological transitions. Theoretical Ecology. Oxford University Press. 2020:263–84. https://doi.org/10.1093/oso/9780198824282.003.0015
38. O'Regan SM, Burton DL. How Stochasticity Influences Leading Indicators of Critical Transitions. Bull Math Biol. 2018;80(6):1630–54. https://doi.org/10.1007/s11538-018-0429-z PMID: 29713924
39. O'Regan SM, O'Dea EB, Rohani P, Drake JM. Transient indicators of tipping points in infectious diseases. J R Soc Interface. 2020;17(170):20200094. https://doi.org/10.1098/rsif.2020.0094 PMID: 32933375
40. O'Regan SM, Lillie JW, Drake JM. Leading indicators of mosquito-borne disease elimination. Theor Ecol. 2016;9:269–86. https://doi.org/10.1007/s12080-015-0285-5 PMID: 27512522
41. Althouse BM, Lessler J, Sall AA, Diallo M, Hanley KA, Watts DM, et al. Synchrony of sylvatic dengue isolations: a multi-host, multi-vector SIR model of dengue virus transmission in Senegal. PLoS Negl Trop Dis. 2012;6(11):e1928. https://doi.org/10.1371/journal.pntd.0001928 PMID: 23209867
42. Focks DA, Daniels E, Haile DG, Keesling JE. A simulation model of the epidemiology of urban dengue fever: literature analysis, model development, preliminary validation, and samples of simulation results. Am J Trop Med Hyg. 1995;53(5):489–506. https://doi.org/10.4269/ajtmh.1995.53.489 PMID: 7485707
43. Anderson RA, Roitberg BD. Modelling trade-offs between mortality and fitness associated with persistent blood feeding by mosquitoes. Ecol Lett. 1999;2:98–105. https://doi.org/10.1046/j.1461-0248.1999.22055.x
44. Petrucciani A, Yu G, Ventresca M. Multi-season transmission model of Eastern Equine Encephalitis. PLoS One. 2022;17(8):e0272130. https://doi.org/10.1371/journal.pone.0272130 PMID: 35976903
45. Wu SL, Marshall JM, Simon SP, Etienne B. Spraying of male mating swarms as a novel vector control intervention: Insights from a mathematical model. AMERICAN. 2017.
46. Wu SL, Henry JM, Citron DT, Mbabazi Ssebuliba D, Nakakawa Nsumba J, Sánchez C HM, et al. Spatial dynamics of malaria transmission. PLoS Comput Biol. 2023;19(6):e1010684. https://doi.org/10.1371/journal.pcbi.1010684 PMID: 37307282
47. Wu SL, Sánchez C HM, Henry JM, Citron DT, Zhang Q, Compton K, et al. Vector bionomics and vectorial capacity as emergent properties of mosquito behaviors and ecology. PLoS Comput Biol. 2020;16(4):e1007446. https://doi.org/10.1371/journal.pcbi.1007446 PMID: 32320389

48. Kiware SS, Chitnis N, Tatarsky A, Wu S, Castellanos HMS, Gosling R, et al. Attacking the mosquito on multiple fronts: Insights from the Vector Control Optimization Model (VCOM) for malaria elimination. PLoS One. 2017;12(12):e0187680. https://doi.org/10.1371/journal.pone.0187680 PMID: 29194440
49. Ryan SJ, McNally A, Johnson LR, Mordecai EA, Ben-Horin T, Paaijmans K, et al. Mapping Physiological Suitability Limits for Malaria in Africa Under Climate Change. Vector Borne Zoonotic Dis. 2015;15(12):718–25. https://doi.org/10.1089/vbz.2015.1822 PMID: 26579951
50. Kraemer MUG, Reiner RC Jr, Brady OJ, Messina JP, Gilbert M, Pigott DM, et al. Past and future spread of the arbovirus vectors Aedes aegypti and Aedes albopictus. Nat Microbiol. 2019;4(5):854–63. https://doi.org/10.1038/s41564-019-0376-y PMID: 30833735
51. Lessler J, Cummings DAT. Mechanistic Models of Infectious Disease and Their Impact on Public Health. Am J Epidemiol. 2016;183:415–22. https://doi.org/10.1093/aje/kww021
52. Lambrechts L, Paaijmans KP, Fansiri T, Carrington LB, Kramer LD, Thomas MB, et al. Impact of daily temperature fluctuations on dengue virus transmission by Aedes aegypti. Proc Natl Acad Sci U S A. 2011;108(18):7460–5. https://doi.org/10.1073/pnas.1101377108 PMID: 21502510
53. Carrington LB, Armijos MV, Lambrechts L, Scott TW. Fluctuations at a low mean temperature accelerate dengue virus transmission by Aedes aegypti. PLoS Negl Trop Dis. 2013;7(4):e2190. https://doi.org/10.1371/journal.pntd.0002190 PMID: 23638208
54. McGregor BL, Kenney JL, Connelly CR. The Effect of Fluctuating Incubation Temperatures on West Nile Virus Infection in Culex Mosquitoes. Viruses. 2021;13(9):1822. https://doi.org/10.3390/v13091822 PMID: 34578403
55. Paaijmans KP, Blanford S, Bell AS, Blanford JI, Read AF, Thomas MB. Influence of climate on malaria transmission depends on daily temperature variation. Proc Natl Acad Sci U S A. 2010;107(34):15135–9. https://doi.org/10.1073/pnas.1006422107 PMID: 20696913
56. Alto BW, Wiggins K, Eastmond B, Ortiz S, Zirbel K, Lounibos LP. Diurnal Temperature Range and Chikungunya Virus Infection in Invasive Mosquito Vectors. J Med Entomol. 2018;55(1):217–24. https://doi.org/10.1093/jme/tjx182 PMID: 29040730
57. Brown JJ, Pascual M, Wimberly MC, Johnson LR, Murdock CC. Humidity - The overlooked variable in the thermal biology of mosquito-borne disease. Ecol Lett. 2023;26(7):1029–49. https://doi.org/10.1111/ele.14228 PMID: 37349261
58. Whittle P. The Outcome of a Stochastic Epidemic--A Note on Bailey's Paper. Biometrika. 1955;42(1/2):116. https://doi.org/10.2307/2333427
59. Mordecai EA, Paaijmans KP, Johnson LR, Balzer C, Ben-Horin T, de Moor E, et al. Optimal temperature for malaria transmission is dramatically lower than previously predicted. Ecol Lett. 2013;16(1):22–30. https://doi.org/10.1111/ele.12015 PMID: 23050931
60. Randolph SE, Green RM, Peacey MF, Rogers DJ. Seasonal synchrony: the key to tick-borne encephalitis foci identified by satellite data. Parasitology. 2000;121 (Pt 1):15–23. https://doi.org/10.1017/s0031182099006083 PMID: 11085221
61. Greenman JV, Benton TG. The amplification of environmental noise in population models: causes and consequences. Am Nat. 2003;161(2):225–39. https://doi.org/10.1086/345784 PMID: 12675369
62. Altizer S, Dobson A, Hosseini P, Hudson P, Pascual M, Rohani P. Seasonality and the dynamics of infectious diseases. Ecol Lett. 2006;9(4):467–84. https://doi.org/10.1111/j.1461-0248.2005.00879.x PMID: 16623732
63. Boyce MS, Haridas CV, Lee CT, The Nceas Stochastic Demography Working Group. Demography in an increasingly variable world. Trends Ecol Evol. 2006;21(3):141–8. https://doi.org/10.1016/j.tree.2005.11.018 PMID: 16701490
64. Tanaka H. Stochastic differential equations with reflecting boundary condition in convex regions. Hiroshima Math J. 1979;9(1). https://doi.org/10.32917/hmj/1206135203
65. van den Driessche P, Watmough J. Reproduction numbers and sub-threshold endemic equilibria for compartmental models of disease transmission. Math Biosci. 2002;180:29–48. https://doi.org/10.1016/s0025-5564(02)00108-6 PMID: 12387915
66. Diekmann O, Heesterbeek JA, Metz JA. On the definition and the computation of the basic reproduction ratio R0 in models for infectious diseases in heterogeneous populations. J Math Biol. 1990;28(4):365–82. https://doi.org/10.1007/BF00178324 PMID: 2117040
67. Yang X. A new numerical scheme for a class of reflected stochastic differential equations. Monte Carlo Methods and Applications. 2013;19(4). https://doi.org/10.1515/mcma-2013-0011
68. Britton T, Lindenstrand D. Epidemic modelling: aspects where stochasticity matters. Math Biosci. 2009;222(2):109–16. https://doi.org/10.1016/j.mbs.2009.10.001 PMID: 19837097
69. Feng Z, Glasser JW, Hill AN. On the benefits of flattening the curve: A perspective. Math Biosci. 2020;326:108389. https://doi.org/10.1016/j.mbs.2020.108389 PMID: 32473161
70. Ferguson NM, Cummings DAT, Fraser C, Cajka JC, Cooley PC, Burke DS. Strategies for mitigating an influenza pandemic. Nature. 2006;442(7101):448–52. https://doi.org/10.1038/nature04795 PMID: 16642006
71. Bezanson J, Edelman A, Karpinski S, Shah VB. Julia: A Fresh Approach to Numerical Computing. SIAM Rev. 2017;59(1):65–98. https://doi.org/10.1137/141000671
72. R Core Team. The R Project for Statistical Computing. https://www.R-project.org/. 2021. Accessed 2024 November 30.